On polyamide 6-montmorillonite nanocomposites obtained by in-situ polymerization

Orietta Monticelli,[1]* Zenfira Musina,[1] Francesca Ghigliotti,[1] Saverio Russo,[1] Valerio Causin[2]

[1]*Dipartimento di Chimica e Chimica Industriale, Università di Genova and INSTM NIPLAB Centre, Via Dodecaneso, 31, 16146 Genova, Italy, fax: +39 010 3536198; email: orietta@chimica.unige.it
[2]Dipartimento di Scienze Chimiche, Università di Padova and INSTM Padova research unit, Via Marzolo, 1, 35131 Padova, Italy.

Abstract: Nanocomposites based on polyamide 6 (PA6) and montmorillonite-type (MMT) commercial clays, either unmodified or organically modified, were prepared by in-situ polymerization of ε-caprolactam (CL). The above materials were characterized in detail by a number of experimental techniques, including transmission electron microscopy (TEM), wide angle X-ray diffraction (WAXD), infrared spectroscopy (FTIR) and differential scanning calorimetry (DSC).
The formation of nanostructured systems was checked not only for the commonly used ω-aminoacid-modified clay, but also for other types of organoclays. In general, a correlation was found between nanoscopic swelling of the clay in molten CL, measured by X-ray diffraction, and level of clay dispersion in PA6. Specifically, with the most swellable clays, completely exfoliated nanocomposites were obtained. However, also layered silicates modified by compatibilizers having carboxy groups, because of the active role of latter in CL polymerization, formed delaminated nanocomposites despite their low degree of swelling in CL monomer.
Both molecular mass and crystallinity of the polyamide matrix were found to be strongly influenced by the presence of specific layered silicates. In particular, some characterization techniques (WAXD, FTIR) have evidenced a close relationship between the MMT used and PA6 crystal structure. Namely, PA6 γ-form is promoted by clay with compatibilizer bearing the carboxy group, which is able to induce the polymer to be tethered on the silicate layers, thus provoking conditions of restricted mobility to occur.

Introduction

Since the early 90s of the past century, after the pioneering research work of Toyota group [1-3] devoted to the preparation and characterization of nanocomposites based on layered silicates and polyamide 6, a lot of publications have appeared in this field both from academia and from industrial research labs.

The above nanocomposites have been prepared by either melt intercalation or in situ polymerization methods. Although the former approach is in general compatible with current industrial processes such as extrusion and injection molding, as far as nanocomposites based on PA6 are concerned, in-situ CL polymerization has been preferably adopted and extensively studied for its easiness. In this latter approach, the layered silicate is preliminarily swollen by the liquid monomer or a monomer solution, so that during subsequent polymerization polymer formation can occur between the intercalated sheets [4]. Specifically, the CL hydrolytic polymerization is

1

promoted by a suitable organic initiator, introduced by cation exchange in the interlayer before the CL swelling step. So far, the attention has been focused on layered silicates modified by an organic compatibilizer of the ϖ-aminoacid type, which is also able to start CL polymerization and produce, in some specific conditions, nanostructured composite material. A different approach has been proposed by Kojima *et al.* [5], who showed that intercalative polymerization of ε-caprolactam could be realized in one pot without making the layered silicate surface organophilic. The above authors reported that, before starting the polymerization, the CL monomer was directly intercalated in Na-MMT water solution in the presence of hydrochloric acid. At high temperature (260 °C), in the presence of excess ε-caprolactam, the so-modified clay could be swollen again, allowing the ring-opening polymerization to proceed in the presence of ε-aminocaproic acid added as a reaction initiator.

Nanocomposites based on PA6 and clays, prepared by both in-situ polymerization or melt intercalation, show many interesting properties. Various authors have reported that PA6 nanocomposites, characterised by exfoliated structures, exhibit a relevant improvement of the mechanical properties [2, 6-8]. Furthermore, layered silicate nanodispersion in PA6 leads to an enhancement of fire retardancy and gas barrier properties [9]. Together with the above features, the crystallinity of the polymer matrix also turned out to be greatly affected by the presence of clay [3, 10-14].

Despite the relevant technological interest for PA6/clay nanocomposites, especially by the in-situ polymerization approach, not much attention has been paid so far to study in detail the influence of organically-modified layered silicate (OMLS) characteristics, such as its surface energy, type and structure of organic modifier and so on, on end properties of these materials in terms of both matrix molecular mass and crystallinity, and level of clay dispersion.

On this basis, in the present work five commercial MMT-type organoclays, characterized by different organic modifiers, have been used in the in-situ polymerization of CL. The characteristics of the resultant material have been evaluated by various characterization techniques and compared to the behaviour of PA6 nanocomposites prepared from unmodified clay.

Results and discussion

Our investigation on the preparation and characterization of nanocomposites based on PA6 and organoclays has been preliminarily focused on the comparison between Nanofil 784[®] (Süd Chemie product), a layered silicate modified by an ϖ-aminoacid, and other commercial clays (from Southern Clay), either unmodified or organically modified, all listed in Table 6, as mentioned in the Experimental.

In order to evaluate the specific influence of the inorganic filler chosen on the material end properties, neat PA6 samples have been prepared using the same polymerization conditions (time, temperature, reactant composition) applied in the nanocomposite syntheses. In agreement to the literature results by Toyota researchers [1-3], X-ray diffraction and TEM characterization data of PA6/Nanofil 784[®] system show the formation of nanostructured material. Indeed, the disappearance of the (001) diffraction peak (Fig. 1), together with the presence of layers showing dispersion of delaminated individual sheets in TEM micrographs (Fig. 2), fully support the formation of an exfoliated nanocomposite.
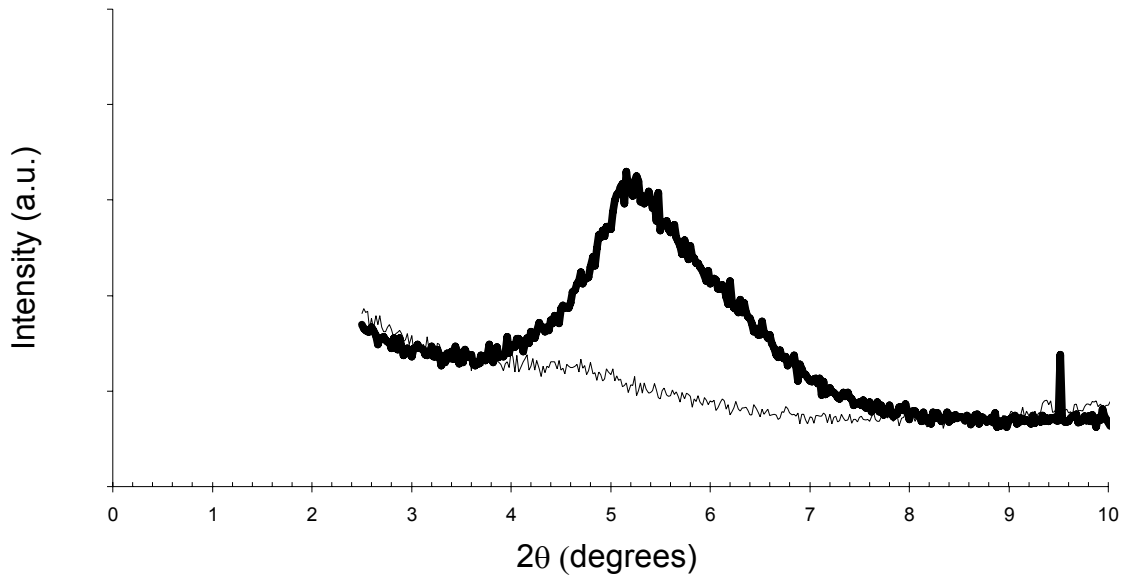
2

Fig. 1. X-ray diffraction patterns of Nanofil 784® (—) and nanocomposite sample PA6N784(3) (—) from 2.5° to 10° of 2θ.
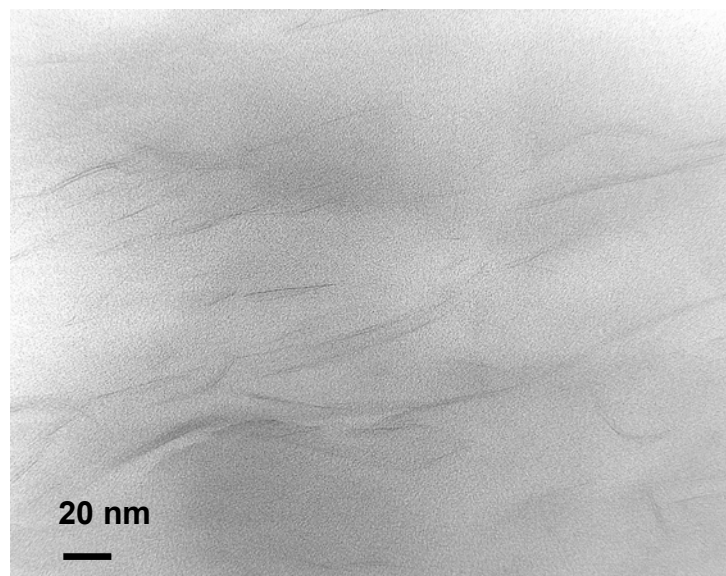

Fig. 2. TEM micrograph of the sample PA6N784(3).

The MMT concentration in the reaction mixture turned out to be a key parameter which has to be strictly controlled in order to obtain a proper clay distribution. Indeed, a rather poor dispersion of layered silicate in PA6 matrix has been obtained when Nanofil 784® amount was doubled (from 5 to 10 wt.-%). Moreover, as will be commented further on, composite molecular masses decreased when increasing the filler content.

Besides studying the level of clay dispersion in PA6, the influence of the organoclay and the corresponding compatibilizer on specific polymer features, such as its molecular mass, thermal behaviour and crystallinity, has been investigated in order to

3

achieve a thorough overview on material properties. Namely, the comparison of molecular masses between neat polyamide and nanocomposite samples has been performed by solution viscosity measurements in H_2SO_4 at 20 °C.

M_w has been calculated by the following equation [15]:

$$[\eta] = 0{,}51 \; 10^{-3} \; M_w^{0.74}$$ (1)

Before accomplishing the above characterization, it has been verified that the layered silicate had very little influence on the polymer viscosity, by comparing the η values of solution containing only PA6 to the values of solutions prepared by mixing PA6 with the proper amount of clay.

Tab. 1. Characterization data of neat PA6 and nanocomposites based on Nanofil 784®.

sample code	clay (g)	Temperature (T_P) (°C)	time (t_p) (h)	η_{rel}[a]	$M_w \times 10^3$
PA6N784(1)	1	270	4	2.40	26.3
PA6(1)	-	270	4	2.82	38.4
PA6N784(2)	1	270	6	2.45	28.1
PA6(2)	-	270	6	3.08	42.0
PA6N784(3)	1	250	4	2.46	27.1
PA6(3)	-	250	4	2.47	30.2
PA6N784(4)	1	250	6	2.45	29.0
PA6(4)	-	250	6	2.80	38.3
PA6N784(5)	2	250	4	2.35	25.1
PA6(5)	-	250	4	2.47	29.8

polymerization conditions: CL=20 g, ACA = 0.8 g
[a] 1 wt % concentration in H_2SO_4 at 20 °C

As shown by the data of Table 1, the addition of layered silicate affects the polyamide molecular mass by restraining its growth, without any further significant influence linked to the variation of reaction parameters, such as time and temperature, contrary to what happens in the neat polymerizing system.

The effect of MMT, organically modified by ω-aminoacid, on the macromolecular growth has been attributed by Usuki *et al.* [2] to the carboxy end groups of the organic modifier, which acts as a polymer chain stopper.

From the aforementioned references [1-3], it also results that the molecular structure of the clay compatibilizer, namely the length of its chain and the presence of COOH groups, is crucial for the mechanism of nanocomposite formation. Indeed, it is well known that COOH groups are capable of affecting both the ring opening reaction and the polyaddition step during PA6 formation. Moreover, the capability of the clay to be swollen by molten CL has been linked to both the number of carbon atoms of the ϖ-amino acid and the active role of carboxy functional groups in the polymerization process. Another important aspect, related to the compatibilizer structure, is that the resultant polyamide chain is ionically bonded to the silicate layers, thus strongly influencing several material end features such as its mechanical properties, thermal decomposition, and so on.

However, the formation of completely exfoliated nanocomposites has also been found when using organoclays of the MMT-type containing modifiers without carboxy

functional groups. As an example, Figures 3 and 4 show the X-ray diffraction pattern and TEM micrograph, respectively, of a composite sample based on PA6 and Cloisite 30B®, prepared using the conditions previously described. Both sets of data show the formation of an exfoliated nanocomposite.
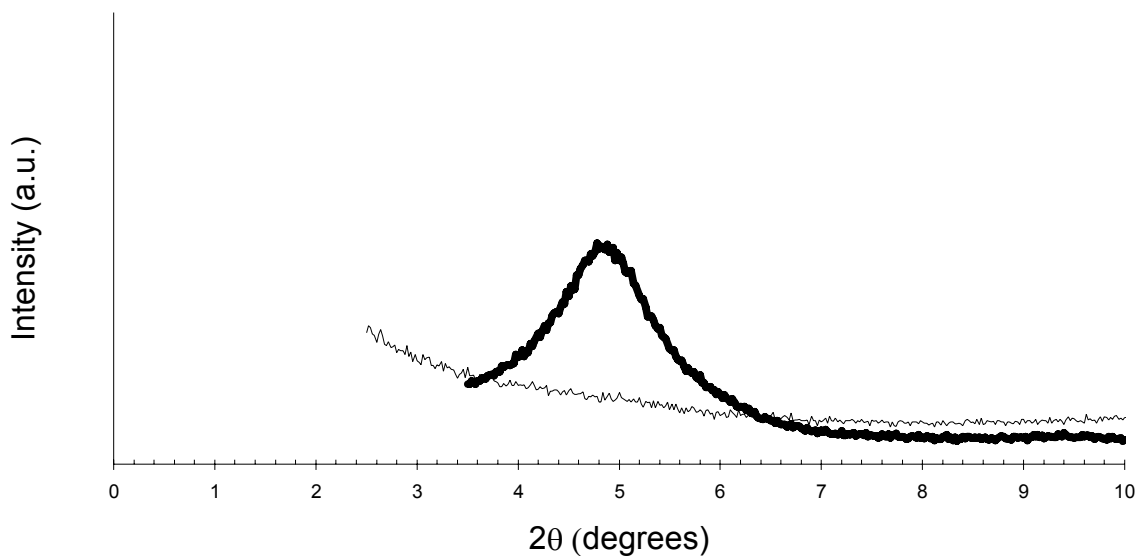

Fig. 3. X-ray diffraction patterns of Cloisite 30B® (—) and nanocomposite sample PA6Cl30B(1) (—) from 2.5° to 10° of 2θ.
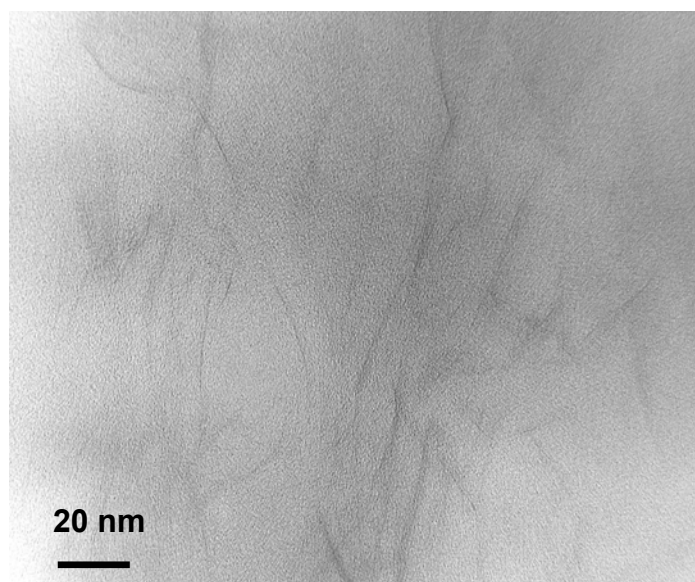

Fig. 4. TEM micrograph of the sample PA6Cl30B(1).

Although the silicate dispersion is similar to that obtained in the composites based on Nanofil 784®, it is important to underline that, using Cloisite 30B® or other organoclays containing compabilizers without carboxy groups, the exfoliation is not accompanied by PA6 chain bonding to the silicate layers. Indeed, the two classes of nanocomposites are expected to be characterized by different properties.

5

As quite often reported [4], clay swelling by CL monomer represents a crucial step of the nanocomposite formation during in-situ polymerization. The possible correlation between the above parameter and the nanocomposite characteristics, in terms of clay dispersion, has been evaluated for the MMT-type organoclays listed in Table 1. The swelling of the layered silicate has been calculated as follows: i) by measuring the basal spacing of the clay, *i.e.* d_{001}, in the X-ray diffraction spectra, before and after its dispersion in the monomer, a difference attributed to the nanoscopic swelling; ii) from Eq. 3, where V_c represents the volume of the dry powder while V_s is defined as the volume of the slurry, *i.e.* the sedimented volume of swollen nanoclay in CL measured after 4 h at 100 °C.

$$S=(V_s-V_c)/V_c \tag{3}$$

With the above equation macroscopic swelling is determined.

Tab. 2. Macroscopic swelling factor and WAXD characterization data of neat clays and clays swollen by molten CL (T=100°C).

sample code	S, macroscopic swelling factor[a]	d_{001} (nm)	Δd_{001}, nanoscopic swelling factor	Type of nanocomposites
Nanofil 784®	10	1.7	0.2	exfoliated
Cloisite 15A®	10	3.4	0.4	exfoliated
Cloisite Na®	7	1.2	0.7	intercalated
Cloisite 93 A®	13	2.5	0.9	intercalated (nearly exfoliated)
Cloisite 20A®	13	2.6	1.2	exfoliated
Cloisite 30 B®	15	1.8	1.6	exfoliated

[a] $S=(V_s-V_c)/V_c$ V_c=volume of the dry powder, V_s = volume of the slurry
[b] Δd_{001} = $d_{\text{clay in molten CL}}$ − $d_{\text{neat clay}}$

It is evident from the data given in Table 2 that a direct correlation between the two swelling parameters (macro and nano) does not exit. The macroswelling, recently studied by Gérard *et al.* [16] in systems composed by organoclays and solvents, has been by these authors attributed to the formation of a gel made of tactoids not necessarily swollen in the interlayer galleries.

On this basis, in order to evaluate the real extent of CL monomer intercalation into the silicate layers, only the nanoscopic swelling measured by X-ray diffraction has to be considered.

As shown by the last two columns of Table 3, in general a good correlation between the above parameter and the layered silicate dispersion in PA6 has been found; namely, completely exfoliated nanocomposites have been obtained with the most swellable clays. Nanocomposite samples based on Cloisite 15A® and Nanofil 784® deserve a more detailed comment. For the above phyllosilicates, the clay dispersion does not follow the degree of swelling; as much as completely exfoliated nanocomposites are obtained despite their low degree of swelling in CL monomer.

The likely explanation of the above behaviour is different for the two clays. As far as Cloisite 15A® is concerned, the large interlayer distance of the original layered silicate (3.4 nm) helps promoting an easy CL diffusion into the galleries, favouring the formation of completely exfoliated structures even in absence of any relevant

swelling. Conversely, Nanofil 784$^®$ which contains an ϖ-aminoacid known to play an active role in the polymerization process by its carboxy groups, forms delaminated nanocomposites as the polyamide chain is directly tethered on the silica layer and, as a consequence, drives the delamination process. It is worth pointing out that also Cloisite Na$^®$, although it does not hold a compatibilizer capable to make it organophilic, is able to swell in CL monomer and form intercalated nanocomposites.

We can conclude that, together with other parameters, the knowledge of nanoscopic swelling of the used clay in CL monomer, can give a preliminary indication of the resultant filler dispersion in the polyamide matrix.

As previously reported, molecular masses of both nanocomposites and neat PA6 have been evaluated by solution viscosity measurements. These data, listed in Table 3, clearly show a decrease of the nanocomposite M_w with respect to that of neat polyamide 6.

Tab. 3. Characterization data of neat PA6 and nanocomposites based on MMT-type clays.

sample code	clay	η_{rel}[a]	$M_w \times 10^3$	high polymer yield (wt/wt)%
PA6(3)	-	2.47	30.2	82
PA6N784(3)	Nanofil 784$^®$	2.46	27.1	85
PA6Cl30B(1)	Cloisite 30 B$^®$	2.20	23.3	81
PA6ClNa(1)	Cloisite Na$^®$	2.28	26.6	82
PA6Cl93A(1)	Cloisite 93A$^®$	2.33	24.9	72
PA6Cl15A(1)	Cloisite 15 A$^®$	2.30	24.8	78
PA6Cl20A(1)	Cloisite 20 A$^®$	2.34	24.9	79

polymerization conditions: CL=20 g, ACA=0.8 g, clay=1 g, t_p=4 h, T_p=250 °C. [a] 1 wt % concentration in H_2SO_4 at 20 °C

The M_w decrease is present not only in the exfoliated, but also in the intercalated nanocomposites (*cfr.* sample PA6ClNa(1) containing Cloisite Na$^®$). On the contrary, molecular masses of microcomposite samples, obtained when the less favourable dispersion conditions are active, turned out to be comparable with those of neat PA6. Taking into account the above finding, it is possible to infer that M_w reduction is mainly related to nanostructure formation.

In order to further elucidate this phenomenon and prove the active role of clays, either unmodified or organically modified, in the polymerization process, additional syntheses have been accomplished using either a reaction mixture without ACA or strongly drying the layered silicate in the reaction vessel before adding the reaction mixture and starting the polymerization.

As expected, when the reaction mixture does not contain ε-amino caproic acid, only by using Nanofil 784® it has been possible to obtain some PA6, although characterized by low yields and rather low M_w values (Table 4). Evidently, the -COOH groups of the clay compatibilizer can play an active role in CL polymerization.

Tab. 4. Characterization data of neat PA6 and nanocomposites based on MMT-type clays.

sample code	clay	time (t_p) (h)	$M_w \times 10^3$	high polymer yield (wt/wt)%
PA6(6)	-	4	-	-
PA6N784(6)	Nanofil 784®	4	7.9	15
PA6N784(7)	Nanofil 784®	6	8.6	
PA6Cl30B(2)	Cloisite 30 B®	4	<5	11
PA6Cl93A(2)	Cloisite 93A®	4	<5	7
PA6ClNa(2)	Cloisite Na®	4	-	-
PA6Cl15A(2)	Cloisite 15 A®	4	-	-
PA6Cl20A(2)	Cloisite 20 A®	4	-	-

polymerization conditions: CL=20 g, ACA=0 g, clay=1g, T_p=250 °C

In principle, also water, entrapped into silicate galleries, might be able to catalyze the ring-opening reaction of CL, leading to a decrease of the polymer molecular mass linked to water concentration. As said above, although clay drying has been carried out directly in the polymerization reactor at 150 °C for 12 hours, no change in the M_w of nanocomposite samples has been found. Higher dehydration temperatures were not adopted in order to avoid thermal degradation of the organic compatibilizer.
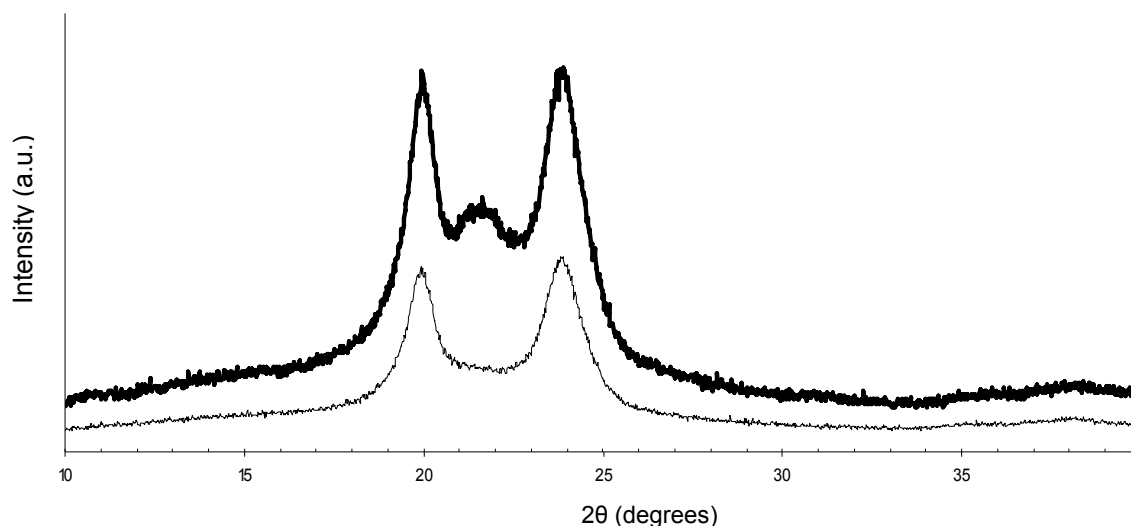

Fig. 5. X-ray diffraction patterns of nanocomposite samples PA6N784(3) (━) and PA6Cl30B(1) (─) from 10° to 37° of 2θ.

On the basis of all above results, in order to fully explain the above phenomenon, other features of the clay/polymer system have to be considered, such as specific interactions of the growing polyamide chain with the silicate layers, role of structural water (which is not removed during the dehydration process), polymer chain restraint

8

caused by its growth into clay galleries, and so on. Namely, the decrease of polyamide molecular mass may be caused by compatibilizer thermal degradation, which is already relevant at T_p of 250 °C. The above degradation has been studied by Fornes *et al.* [17], who checked polymer matrix degradation and colour formation in PA6/organoclay nanocomposites formed by melt blending. The kind of polyamide used, as well as the chemical structure of organoclay surfactant, affected the extent of polymer degradation, namely its molecular mass decrease, and colour generation. The specific influence of compatibilizer thermal decomposition on polymer matrix features has been recently analyzed in a work of ours [18].

As previously quoted, another aspect, extensively studied by many authors, is the influence of silicate platelets on the crystal structure of PA6 matrix in nanocomposites prepared by either in situ polymerization or melt processing [3, 10-14,19]. Since the first investigations it was reported that, when the platelets of montmorillonite are dispersed in polyamide 6, the presence of polymer γ form is enhanced [3, 11]. More recently, various characterization techniques (*e.g.* DSC, FTIR, and WAXD) have been applied in order to better elucidate the role of dispersed silicates on PA6 crystalline structure. VanderHart *et al.* [13] pointed out that silicate layers promote the γ-form, regardless of the formation pathway, and γ-crystallites dwell near the polyamide/clay interface. The above authors concluded that the layered silicate affects PA6 crystal structure under γ-favoring conditions such as rapid cooling, conditions of restricted mobility, *etc.* As the effect of cooling on PA6 crystal formation is well known [13]; all our samples have been cooled in the same way in order to assess the real influence of clay on crystallization behaviour of the polymer matrix.

Figure 5 shows the X-ray diffraction patterns of two nanocomposites based on Cloisite 30B® and Nanofil 784®, respectively.

It is evident that PA6 crystal structure is linked to the specific layered silicate used, namely on its modifier. While Nanofil 784®, containing a compatibilizer with carboxy groups, promotes γ-form, only α-form is produced using Closite 30B®. Furthermore, as shown in Fig. 6, γ-form of composites based on Nanofil 784® increases by increasing the clay concentration in the reaction mixture.

Apart from the sample based on Cloisite 93 A® all composites, which do not contain a compatibilizer with carboxy groups, are characterized by PA6 α-crystallites. Taking into account the above results, it seems that polyamide γ-form is favoured only when the polymer chains are anchored to the silicate layers, namely when conditions of restricted mobility occur. Unfortunately, thermal transition temperatures, determined by DSC, have not been able to further support the above findings, as no significant differences were detected for all samples analyzed.

Our results do not seem to agree with the findings quoted in the aforementioned references. However, it is necessary to take in account that most clays, listed in the above papers and used in the in-situ CL polymerization, contain a carboxy compatibilizer, which chemically interacts with PA6 chains, as explained previously.

The peculiar behaviour of Closite 93 A®, namely the formation of a small γ-form of the resultant nanocomposites and its catalytic effect in CL spontaneous polymerization, needs to be further studied by additional measurements, mainly focused on clay composition and structure, presence of impurities, organic compatibilizer thermal decomposition, and so on.
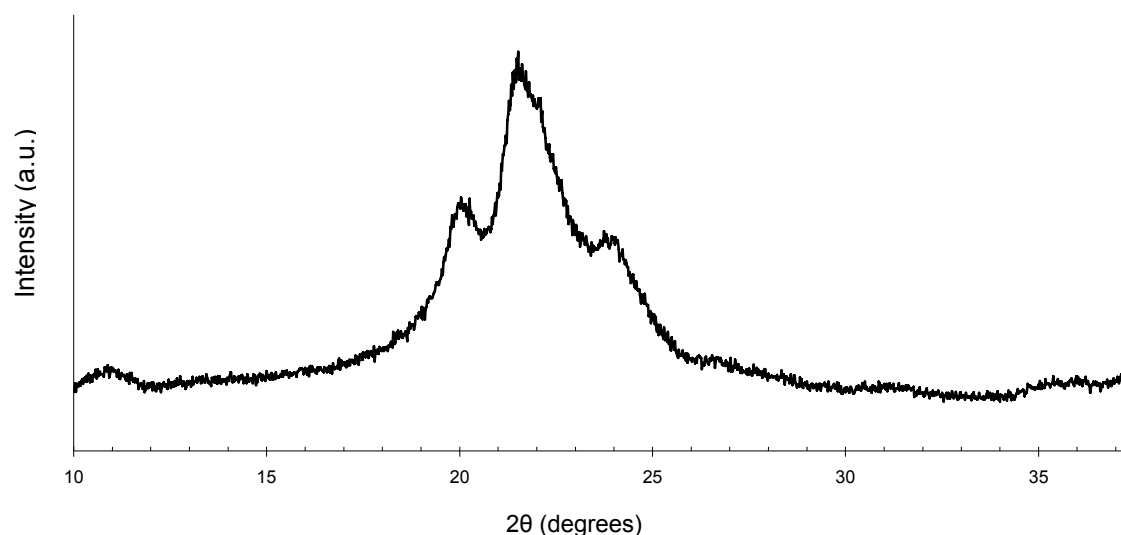
Fig. 6. X-ray diffraction pattern of nanocomposite sample PA6N784(5) from 10° to 37° of 2θ.

For a better understanding of the above phenomenon, PA6 crystal structure for all other nanocomposites have been investigated (Table 5).

Tab. 5. Crystalline forms of neat PA6 and nanocomposites based on MMT-type clays.

sample code	clay	crystalline form
PA6	-	α
PA6N784(3)	Nanofil 784[®]	$\alpha+\gamma$
PA6Cl15A(1)	Cloisite15A[®]	α
PA6ClNa(1)	Cloisite Na[®]	α
PA6Cl93A(1)	Cloisite 93 A[®]	$\alpha+$(small γ)
PA6Cl20A(1)	Cloisite 20A[®]	α
PA6Cl30B(1)	Cloisite 30 B[®]	α

Besides WAXD characterization, FTIR has been applied to study the influence of clay on polyamide crystalline form. The above technique can be used to support X-ray diffraction measurements, being possible both to distinguish between γ- and α-form bands [20] and to give an indication on macromolecular interactions [21].

Four samples have been analyzed: neat PA6, PA6/Cloisite Na[®], PA6/Cloisite 30B[®] and PA6/Nanofil 784[®]. Comparing the IR spectra of the above samples, it results that bands typical of polyamide γ-form (975 cm^{-1} CO-NH in plane vibration, 1235 cm^{-1} twist-wag vibration and 1438 cm^{-1} CH$_2$ scissor vibration) are present only in the nanocomposite based on Nanofil 784[®], thus confirming WAXD results (Fig. 7a).

Furthermore, it is interesting to observe (Fig. 7b) that Fermi resonance of NH-stretching (3064 cm^{-1}) shifts towards higher wavenumbers in the sample PA6/Nanofil 784[®] (3094 cm^{-1}).

Indications about the influence of layered silicate on polymer chain interactions can be attained considering the IR region at high wavenumbers (from 4000 to 2500 cm^{-1}). Absorption band of nanocomposite samples, corresponding to the hydrogen-bonded

10

NH vibration mode (between 3300 and 3310 cm^{-1}), appears to be weaker than that of neat PA6. As reported by Wu *et al.* [21], the decrease of absorbance in this peak is caused by silicate layers, which limit the formation of hydrogen-bonded sheets.
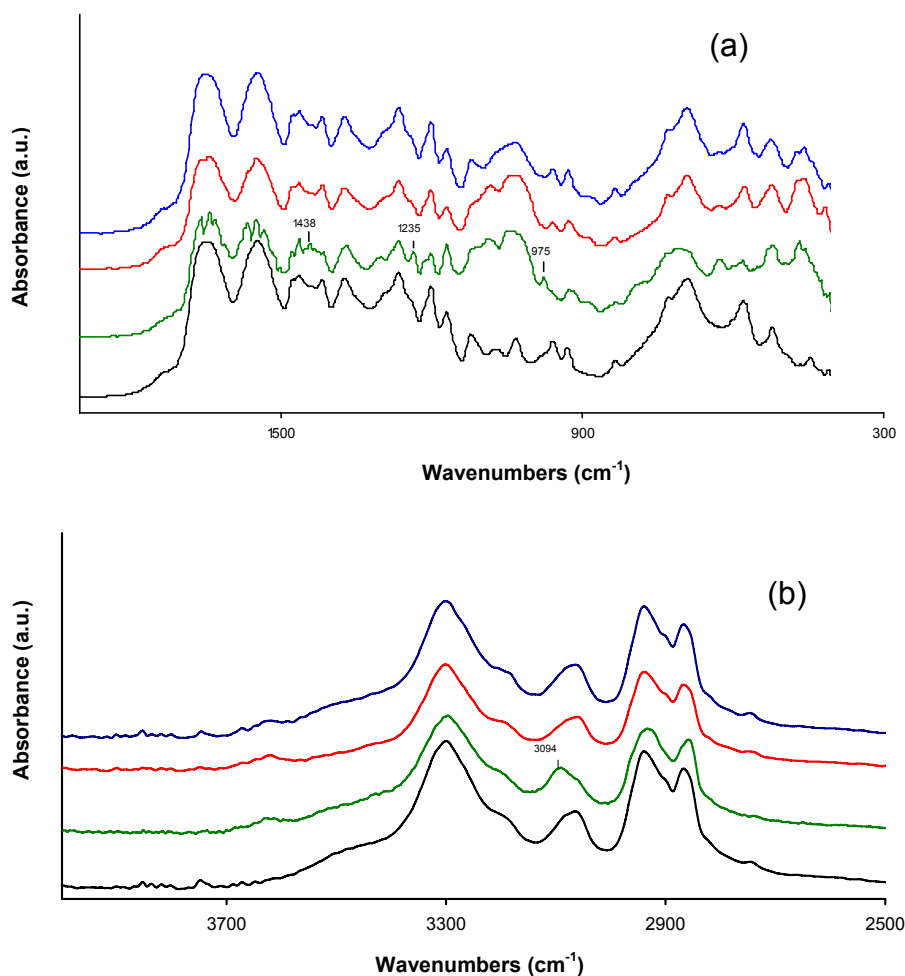

Fig. 7. FTIR spectra of neat PA6 (——) and nanocomposite samples PA6ClNa(1) (PA6/Cloisite Na$^{®}$) (——), PA6N784(3) (PA6/Nanofil 784$^{®}$) (——) and PA6Cl30B(1) (PA6/Cloisite 30B$^{®}$) (——).

Conclusions

Nanocomposites based on PA6 and MMT-type commercial clays, have been prepared by using in-situ polymerization. Firstly, the formation of nanostructured materials has been verified not only by introducing conventional clay modified with an ϖ-aminoacid but also with other organoclays.

As a crucial step of nanocomposite preparation by in-situ polymerization is the swelling of the clay in the monomer, the relationship between the above parameter and the dispersion of the clay in the polymer matrix has been verified using either unmodified or organically modified clays. Although, in general, completely exfoliated nanocomposites have been obtained with the most swellable clays, in the case of layered silicates characterized by a large interlayer distance or containing a ϖ-aminoacid the above rule seems not to be followed, as they give delaminated

11

nanocomposites despite their low degree of swelling in the monomer. Indeed, while in the former system the large dimensions of the distance among the galleries promote an easy CL diffusion, thus favouring the formation of completely exfoliated structures, for the ϖ-aminoacid modified clay, polyamide chain directly tethered on the silica layer might drive the delamination process.
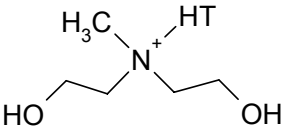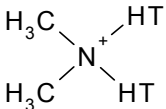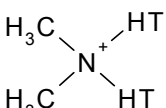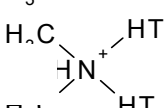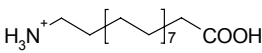
One of the most relevant polymer features which turn out to be affected by the presence of the layered silicate is its molecular mass. Indeed, nanocomposite M_w was found to be lower, as compared to that of neat polyamide 6. It has been guessed that the above phenomenon, specifically related to nanostructured material formation, might be caused by various polymer/clay features such as specific interactions of the growing polyamide chain with the silicate layers, role of the structural water, polymer chain restraints caused by its growth into clay galleries and thermal degradation of the compatibilizer, which is already relevant at T_p of 250 °C.

Finally, also polymorphism has been found to be influenced by the presence of specific layered silicate. In particular, some of the characterization techniques (WAXD and FTIR) have evidenced a correlation between PA6 crystal structure and the layered silicate used. Indeed, it seems that polyamide γ-form is promoted when conditions of restricted mobility occur.

Experimental part

Materials

Tab. 6. Characteristics of montmorillonites used.

trade name	chemical structure of modifying ions	notation for intercalation ions[a]	d_{001}[b] (nm)
Cloisite Na®[c]	-	-	1.17
Cloisite 30B®[c]		MT2EtOH	1.85
Cloisite 15A®[c]		2M2HT	3.15
Cloisite 20A®[c]		2M2HT	2.42
Cloisite 93A®[c]		M2HTH	2.36
Nanofil 784®[d]		H3NC17COOH	1.66

[a]The abbreviations of the quaternary ammonium ions are as follows: M= methyl, B= benzyl, HT= hydrogenated tallow (composed of ~65% C18. ~30% C16. ~5% C14), EtOH= hydroxyethyl. For all clays, Cl⁻ is the corresponding anion; [b] values given by the manufactories; [c] by Southern Clay; [d] by Süd Chemie

ε-Caprolactam, kindly supplied by DSM Research, Geleen, The Nederlands, and ε-aminocaproic acid (ACA, from Fluka) were used as received.

Five montmorillonites (Cloisite Na®, Cloisite 30B®, Cloisite 15A®, Cloisite 20A®, Cloisite 93A®) were supplied by Southern Clay, while Nanofil 784® was provided by Süd Chemie. Apart from Cloisite Na®, all other layered silicates are OMLSs, *i.e.* organoclays, made more or less organophilic by ion exchange of pristine alkali cations with various ammonium salts (Table 6). Cloisite Na® has an exchange capacity of 92.6 meq/100g clay.

Neat PA6 and composite sample preparation

Neat PA6 was synthesized at high temperature (250 °C) using an aluminium block heated by electric resistors connected to a rheostat. Mixtures of CL and ACA were introduced into a glass polymerization vessel, provided with a mechanical stirrer, at room temperature and heated at the polymerization temperature (T_p) by placing the vessel in the aluminium block; typical polymerization time (t_p) was 4 h. At the end of the reaction, the vessel was rapidly cooled to room temperature under a continuous stream of nitrogen.

As far as the preparation of composite material is concerned, prior to the start of ε-caprolactam hydrolytic polymerization at the chosen temperature (T=250 °C), swelling of layered silicates by the molten monomer had been carried out at 100 °C for 1 h. The following polymerization was accomplished using the same procedure described for the polymerization of neat PA6.

A typical reaction mixture was: 20 g of CL, 0.8 g of ACA and 1 g of clay. After polymerization and cooling, all solid samples were broken into small pieces and unreacted caprolactam, higher oligomers and other low mass species were removed by Soxhlet extraction with methanol for 48 h.

Characterization techniques

Solution viscosity of both neat PA6 and hybrid samples was measured in a suspended level Ubbelohde viscometer at 25 °C in 96% H_2SO_4. Wide angle X-ray diffraction (WAXD) patterns were recorded using a Philips PW 1830 powder diffractometer (Ni-filtered Cu Kα radiation). Clay nanoscopic swellings in molten CL were measured by a Philips X'Pert PRO diffractometer (Cu Kα radiation), equipped with an Anton Paar TTK450 temperature control cell.

TEM measurements were performed using a high-resolution transmission electron microscope (JEOL 2010). Ultrathin sections (about 100 nm thick) of material as received after polymerization were cut by a Power TOME X microtome equipped with a diamond knife and placed on a 200-mesh copper grid.

FT-IR spectra were recorded on a Bruker IFS66 spectrometer. The KBr pellets were prepared by mixing the sample with KBr powder (around 1:100) and using a hydraulic press at the pressure of 10 tonnes. All the samples were dried at 120 °C for 4 h under inert atmosphere and were scanned in the range 400-4000 cm^{-1} with nitrogen purge.

Differential Scanning Calorimetry (DSC) analyses were performed on a Mettler calorimetric apparatus, mod. TC10A, at a heating rate of 20 K·min^{-1}.

References

[1] Usuki, A.; Kojima, Y.; Kawasumi, M., Okada, A.; Fukushima, Y.; Kurauchi, T.; Kamigaito, O. *J. Mater. Res.* **1993**, *8*, 1174.

[2] Usuki, A.; Kojima, Y.; Kawasumi, M.; Okada, A.; Fukushima, Y.; Kurauchi, T.; Kamigaito, O. *J. Mater. Res.* **1993**, *8*, 179.

[3] Kojima, Y.; Usuki, A.; Kojima, Y.; Kawasumi, M.; Okada, A.; Fukushima, Y.; Kurauchi, T.; Kamigaito, O. *J. Mater. Res.* **1993**, *8*, 1185.

[4] Sinha, Ray, S.; Okamoto, M. *Prog. Polym. Sci.* **2003**, *28*, 1539 and references quoted therein.

[5] Kojima, Y.; Usuki, A.; Kawasumi, M.; Okada, A.; Kurauchi, T.; Kamigaito, O. *J. Polym. Sci. Part A: Polym. Chem.* **1993**, *31*, 1755.

[6] Wu, S.H.; Wang, F.Y.; Ma, C.-C.M.; Chang, W.C.; Kuo, C.-T.; Kuan, H.-C.; Chen W.-J. *Mater. Lett.* **2001**, *49*, 327.

[7] Fornes, T.D.; Yoon, P.J.; Hunter, D.L.; Keskkula, H.; Paul, D.R. *Polymer* **2002**, *43*, 5915.

[8] Uribe-Arocha P.; Mehler, C.; Puskas, J.E.; Altstadt, V. *Polymer* **2003**, *44*, 2441.

[9] Kashiwagi, T.; Harris Jr. R.H.; Zhang X.; Briber R.M.; Cipriano B.H.; Raghavan S.R.; Awad W.H.; Shields J.R. *Polymer* **2004**, *45*, 881.

[10] Kamal, M.R.; Borse, N.Y.; Garcia-Rejon, A. *Polymer Eng. Sci.* **2002**, *42*, 1883.

[11] Liu, L.; Qi, Z.; Zhu, X. *J. Appl. Polym. Sci.* **1999**, *71*, 1133.

[12] Liu, X.; Wu, Q. *Polymer* **2002**, *43*, 1933.

[13] VanderHart, D.L.; Asano, A.; Gilman, J.W. *Chem. Mater.* **2001**, *13*, 3796.

[14] Fornes, T.D.; Paul, D.R. *Polymer* **2003**, *44*, 3945.

[15] Ueda, K.; Nakai, M.; Hattori, K.; Yamada, K.; Tai, K. *Kobunshi Ronbunshu* **1997**, *56*, 401.

[16] Burgentzlé, D.; Duchet, J.; Gérard, J.F.; Jupin, A.; Fillon, B. *J. Colloid and Inter. Sci.* **2004**, *278*, 26.

[17] Fornes, T.D.; Yoon, P.J.; Paul, D.R. *Polymer* **2003**, *44*, 7545.

[18] Monticelli, O.; Musina, Z.; Frache, A.; Bellocci, F.; Camino, G.; Russo, S. *Polym. Degrad. Stab.* **2007**, *92*, 370.

[19] Homminga, D.S.; Goderis, B.; Mathot, V.B.F.; Groeninckx, G. *Polymer* **2006**, *47*, 1630.

[20] Kyotani, M.; Mitsuhashi, S. *J. Polym. Sci. Part A: Polym. Chem.* **1972**, *10*, 1497.

[21] Wu, Q. ; Liu, X. ; Berglund, L.A. *Polymer* **2002**, *43*, 2445.